Enzymology

DOI: 10.1002/anie.201402679

Chemical Probing of the Human Sirtuin 5 Active Site Reveals Its Substrate Acyl Specificity and Peptide-Based Inhibitors**

*Claudia Roessler, Theresa Nowak, Martin Pannek, Melanie Gertz, Giang T. T. Nguyen, Michael Scharfe, Ilona Born, Wolfgang Sippl, Clemens Steegborn, and Mike Schutkowski**

Abstract: *Sirtuins are NAD^+-dependent deacetylases acting as sensors in metabolic pathways and stress response. In mammals there are seven isoforms. The mitochondrial sirtuin 5 is a weak deacetylase but a very efficient demalonylase and desuccinylase; however, its substrate acyl specificity has not been systematically analyzed. Herein, we investigated a carbamoyl phosphate synthetase 1 derived peptide substrate and modified the lysine side chain systematically to determine the acyl specificity of Sirt5. From that point we designed six potent peptide-based inhibitors that interact with the NAD^+ binding pocket. To characterize the interaction details causing the different substrate and inhibition properties we report several X-ray crystal structures of Sirt5 complexed with these peptides. Our results reveal the Sirt5 acyl selectivity and its molecular basis and enable the design of inhibitors for Sirt5.*

The reversible acetylation of lysine side chains represents one of the most frequent posttranslational modifications in proteins conserved from bacteria to eukaryotes.[1] Acetylation states are regulated by the action of lysine acetyltransferases and lysine deacetylases. One class of lysine deacetylases, the sirtuins, require NAD^+ as a cosubstrate, linking their activity to energy levels of the cell. They transfer the acetyl group from the lysine side chain to the 2′-hydroxyl group of the ADP ribose moiety of NAD^+ under nicotinamide release.[2] Sirtuins are involved in many metabolic and stress response processes, and modulators of human isoforms are interesting drug candidates for aging-related diseases including diabetes, cancer, and neurodegeneration.[3] Some sirtuin isoforms were found to be specific for other acyl modifications on the lysine side chain. Besides acetylation, modifications like propionylation,[4] butyrylation,[4a] crotonylation,[5] malonylation,[6] succinylation,[7] myristoylation,[8] and 3-phosphoglycerylation[9] were detected in vivo. The mitochondrial isoform sirtuin 5 (Sirt5) and the nuclear isoform sirtuin 6 (Sirt6) have a much lower deacetylation activity than several other isoforms.[10] For Sirt6 it could be demonstrated that long acyl chains, such as myristoyl residues, represent much better substrates as a result of improved K_M values,[10b] similar to findings for the *Plasmodium falciparum* sirtuin 2A.[11]

Sirt5 was also found to remove octanoyl and decanoyl residues from model peptides.[12] In particular, this isoform was recently shown to be an effective demalonylase/desuccinylase in vitro[13] and in vivo.[6,13b] Du et al. were able to demonstrate that the change from acetyl to succinyl residues in three different model peptide sequences increased catalytic efficiencies (k_{cat}/K_M) between 75- and 1000-fold but individual K_M and k_{cat} values could not be determined for acetylated substrates.[13a] Crystal structure analysis identified an interaction between the carboxyl function of the succinylated peptide lysine and the Sirt5 side chains of Arg105 and Tyr102,[13a] indicating a mechanism for substrate acyl discrimination. Interestingly, these residues also cause isoforms and substrate acyl specific inhibitor effects.[14] Here we investigated the effects of substrate lysine modifications in a more systematic way and developed novel peptide-based Sirt5 inhibitors through acyl group modifications. As the peptide we used a carbamoyl phosphate synthetase I (CPS1)-derived sequence (**1**) identified through high-density peptide micro-

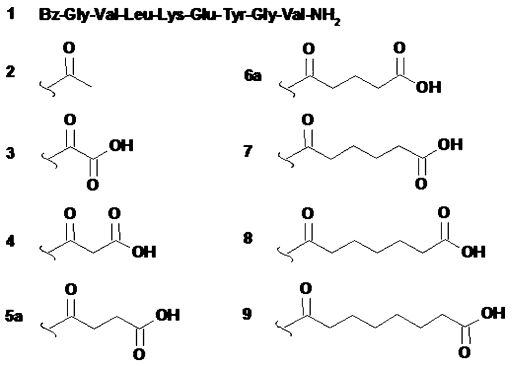

Scheme 1. Homologous row of dicarbonic acyl (**3**–**9**) and acetyl (**2**) residues attached to the lysine side chain of CPS1 peptide **1**.

[*] C. Roessler,[+] Dr. I. Born, Prof. Dr. M. Schutkowski
Department of Enzymology
Institute of Biochemistry and Biotechnology
Martin-Luther-University Halle-Wittenberg
Kurt-Mothes-Strasse 3, 06120 Halle/Saale (Germany)
E-mail: mike.schutkowski@biochemtech.uni-halle.de
T. Nowak,[+] M. Scharfe, Prof. Dr. W. Sippl
Department of Medical Chemistry, Institute of Pharmacy
Martin-Luther-University Halle-Wittenberg
Halle/Saale (Germany)
M. Pannek,[+] Dr. M. Gertz, G. T. T. Nguyen, Prof. Dr. C. Steegborn
Department of Biochemistry, University of Bayreuth (Germany)
[+] These authors contributed equally to this work.

[**] The M.S. research group thanks BMBF (ProNet-T3) for financial support, Željko Simić for synthesis of HMG-modified CPS1 peptide derivative, and Dr. Angelika Schierhorn for MALDI mass spectrometry. The C.S. research group thanks Oberfrankenstiftung. Atomic coordinates and structure factors of the Sirt5–peptide complexes were deposited in the Protein Data Bank under the PDB codes 4UTN, 4UTR, 4UTV, 4UTX, 4UTZ, 4UU7, 4UU8, 4UUA, and 4UUB.

Supporting information for this article is available on the WWW under http://dx.doi.org/10.1002/anie.201402679.

array experiments[1] and shown to serve as a Sirt5 substrate in its acetylated form (Scheme 1).[14a]

In Sirt5 crystal structures Arg105 adopts different conformations suggesting that larger acyl residues might be able to interact with Tyr102 and Arg105, too. Therefore, we synthesized CPS1 substrate analogues acylated at the lysine side chain with oxalyl (**3**), malonyl (**4**), succinyl (**5a**), glutaryl (**6a**), adipoyl (**7**), pimeloyl (**8**), and suberoyl (**9**) residues (Scheme 1). Moreover, we introduced double bonds (**5e**–**5g**), heteroatoms (**6e**–**6g**), and additional substituents to succinyl and/or glutaryl moieties like methyl groups (**5b**, **5c**, **6b**, **6c**, **6g**, and **6d**), methylidene groups (**5e**), hydroxyl groups (**6d**), and amino groups (**5d**). Additionally, we replaced the carboxyl group of the succinyl residue with a nitro function (**5l**) as well as a methyl group (**5n**) (Scheme 2 and Scheme 3). Finally, we introduced larger substituents to the 3-position of succinyl (**5h**–**k** and **5m**) (Scheme 2) and the 4-position of glutaryl residues (**6h**) (Scheme 3).

Kinetic constants for the substrates (Table 1) were determined using an HPLC-based assay. Controls without NAD^+ under identical conditions yielded no conversion of the substrates. Inspection of the kinetic constants uncovers the surprising fact that the introduction of an additional carboxyl group to the acyl chain did not significantly influence

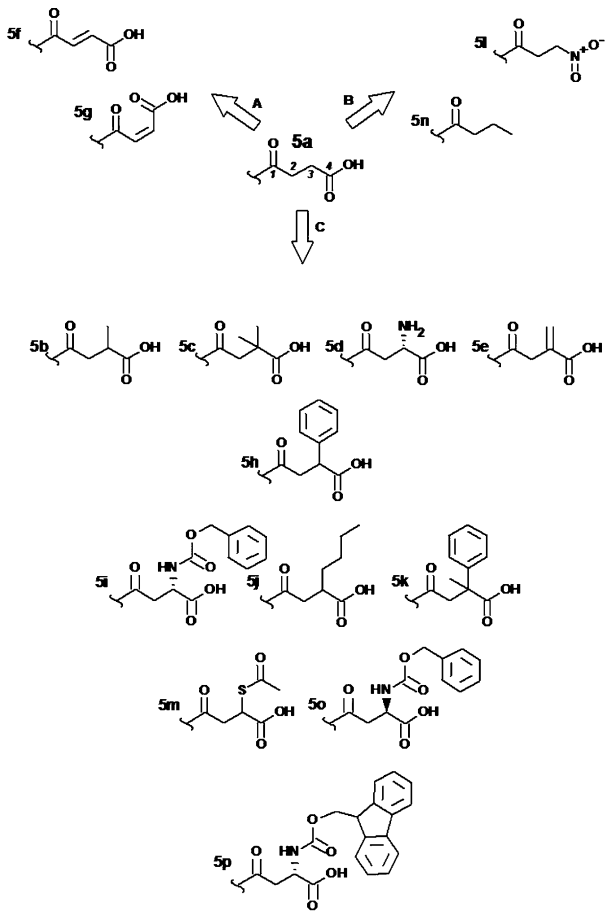

Scheme 2. Derivatization of **5a**: A) dehydrogenation; B) replacement of carboxyl group by methyl or nitro function; C) substitution on C3. **5j** represents a mixture of 2- and 3-butylsuccinyl CPS1.

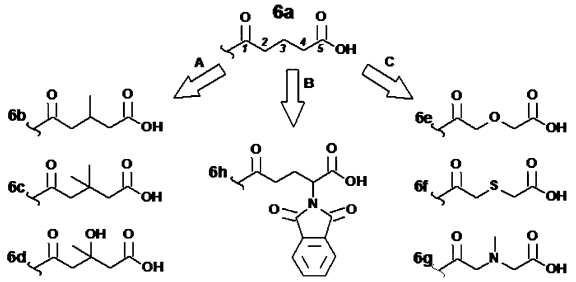

Scheme 3. Derivatization of **6a**: A) substitutions on C3; B) substitutions on C4; C) replacement of the C3-carbon by oxygen, sulfur, or methylated nitrogen.

Table 1: Kinetic constants for differently acylated CPS1-derived peptides.

Compound	K_M [μM]	k_{cat} [s^{-1}]	k_{cat}/K_M [$M^{-1}s^{-1}$]
2	24.3 ± 9.1	$3.9\times10^{-4}\pm6\times10^{-5}$	16
3	415.8 ± 24.3	$1.6\times10^{-3}\pm8\times10^{-5}$	4
4	5.1 ± 1.1	$1.9\times10^{-2}\pm1\times10^{-3}$	3758
5a	3.8 ± 0.6	$5.3\times10^{-2}\pm2\times10^{-3}$	13995
5b	3.1 ± 0.3	$2.4\times10^{-3}\pm4\times10^{-5}$	774
5c	5.3 ± 1.0	$2.2\times10^{-4}\pm8\times10^{-6}$	42
5d	130.3 ± 57.2	$8.4\times10^{-2}\pm2\times10^{-3}$	644
5e	8.2 ± 0.7	$2.5\times10^{-3}\pm5\times10^{-5}$	307
5f	46.7 ± 8.0	$1.7\times10^{-3}\pm1\times10^{-4}$	37
5g	191.8 ± 99.0	$1.5\times10^{-3}\pm5\times10^{-4}$	8
5l	44.8 ± 17.1	$5.2\times10^{-3}\pm8\times10^{-4}$	116
6a	4.1 ± 1.0	$7.7\times10^{-2}\pm2\times10^{-3}$	18699
6b	5.7 ± 0.6	$3.3\times10^{-3}\pm5\times10^{-5}$	579
6c	16.3 ± 3.5	$1.1\times10^{-4}\pm8\times10^{-6}$	7
6d	7.6 ± 0.92	$3.8\times10^{-3}\pm1\times10^{-4}$	500
6e	10.1 ± 2.0	$1.0\times10^{-1}\pm7\times10^{-3}$	9906
6f	2.7 ± 0.5	$2.3\times10^{-2}\pm7\times10^{-4}$	8613
6g	12.1 ± 2.7	$1.6\times10^{-2}\pm1\times10^{-3}$	1325
7	6.5 ± 1.6	$1.0\times10^{-2}\pm6\times10^{-4}$	1538
8	80.5 ± 22.9	$2.8\times10^{-4}\pm4\times10^{-5}$	4
9	409.1 ± 283.0	$5.3\times10^{-4}\pm2\times10^{-5}$	1

the apparent affinity to the active site of Sirt5, as reflected by the almost comparable K_M values for **2** and **4**. Instead, the respective k_{cat} value is increased about 50-fold demonstrating that this modification either influences the velocity or changes the nature of the rate-limiting step of the Sirt5-catalyzed reaction. Insertion of one (**5a**) and two (**6a**) additional methylene groups did not improve the K_M value but increased the k_{cat} value 140-fold and 200-fold, respectively, as compared to **2**. Insertion of an additional methylene group (**7**) yields a substrate with a similar apparent affinity to the active site but 7-fold reduced k_{cat} value compared to **6a**. Insertion of more methylene groups (**8** and **9**) resulted in substrates with k_{cat} values similar to that of **2** and increased K_M values. Replacement of the methyl group of the acetyl residue in **2** by a carboxyl function (**3**) increased the K_M value by more than 15-fold. Molecular docking of **3** shows that the distance between the carboxyl group of **3** and Tyr102 as well as Arg105 is too large for interaction with these residues. Additionally, one oxygen of the carboxyl group of **3** clashes with the backbone carbonyl of Val221 which might explain why the K_M value of **3** is lower than that of **5a** (Figure S9).

Obviously, **4**, **5a**, and **6a** represent most likely physiological substrates for Sirt5; this is reflected by the superior specificity constants k_{cat}/K_M. The very similar apparent affinities, indicated by K_M values, of Sirt5 for **5a** and **6a** could be confirmed by the determination of dissociation constants (K_D) using isothermal titration calorimetry (Figure S8). We found K_D values of 700 ± 50 nM and 710 ± 110 nM for **5a** and **6a**, respectively. The improved turnover of **5a** relative to that of **2** is not simply caused by the increased length of the acyl chain because **5n** showed kinetic constants comparable to those of **2** (data not shown). Introduction of a double bond into the succinyl residue resulted in **5f** and **5g**, which showed an about 30-fold decrease in the turnover. The K_M value is increased about 12-fold for **5f** but by more than 50-fold for **5g** with a *cis*-configured double bond. We compared the structure of the zebrafish Sirt5 (zSirt5)/**5a** complex with docking poses of **5f** and **5g**. Due to the double bond, the acylated lysine residues are forced into a planar orientation, which is not suited to form an optimal hydrogen bond to Tyr102 and a salt bridge to Arg105 (Figure S17).

We solved crystal structures of zSirt5, which is highly homologous to the less reproducibly crystallizing human enzyme (Figure S11), in complex with **5a**, **6a**, and **7** to analyze the binding details of the modifications on the lysine side chain. The final models are composed of two zSirt5 molecules, each complexing one zinc cation. The active site of one molecule is occupied by the respective substrate peptide, with a consistent salt bridge between the carboxyl group of the acyl moiety and Arg101 as well as a hydrogen bond to Tyr98 (Figure 2a), whereas a buffer ion interacts with Arg101 in the active site of the second zSirt5 molecule. In comparison to the succinyl moiety of **5a**, the glutaryl and adipoyl modifications show an increasingly twisted conformation, allowing very similar positions for the distal carboxyl group despite different chain lengths (Figure 1a). The adipoyl modification shows a slight movement toward the catalytic His154 to accommodate the broader, helically arranged carbon chain, resulting in a strained conformation and an elongation of the conserved hydrogen bond between the lysine ε-amino group and the Val217 main-chain carboxyl oxygen. Additional extension of the substrate acyl chain (**8** and **9**) could not be bound in the same mode as for **5a**, **6a**, and **7** by twisting the chain, resulting in the loss of the conserved hydrogen bond to oxygen of Val217 but a similar carboxyl interaction with Arg101/Tyr98.

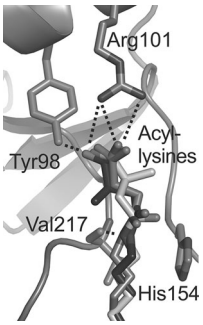

Figure 2. Crystal structures of zSirt5 active-site with superposed **5a** (gray), **5b** (dark gray), and **5c** (light gray). The protein is shown only once for clarity (zSirt5/**5a** complex; gray), since all protein residues superpose well. Polar interactions between active-site residues and substrate peptides' acylated lysine are indicated by dotted lines.

Flexible docking of **8** and **9** indicates that Arg105 changes its conformation to enable similar interactions. This Arg105 conformation is also observed in the Sirt5/thioacetyl-H3K9/CHES complex structure (3RIG), showing that this conformation is possible for the protein. The substrate hydrogen bond to Tyr102 is completely lost, however. This lost interaction and possibly a nonoptimal Arg105 conformation thus appear to be the reasons for the weaker apparent binding and lowered catalytic efficiencies for these substrates. Further extending the acyl chain would lead to a complete loss of the Arg105 interaction and to energetically unfavorable acyl conformations due to limited space within the substrate-binding pocket of Sirt5 (Figure 1b).

Crystal structures of **5a** and **6a** bound to zSirt5 revealed that there is some space around position 3 of the acyl residue and docking studies with **5b**, **5c**, and **6b**, **6c** suggested that they could bind to Sirt5 similar to **5a** and **6a**, respectively. The substituents do not disturb the NAD^+ productive conformation, as suggested by docking studies (Figure S10) and indicated by crystal structure analysis of zSirt5 in complex with **5b** or **5c** (Figure 2). We thus tested single (**5b**, **5e**, **5d**, and **6b**) and double substitutions on this position (**5c**, **6c**, and **6d**) and replacement of the methylene moiety at position 3 by oxygen (**6e**) and sulfur (**6f**), and by methyl-substituted nitrogen (**6g**). Introduction of heteroatoms into the acyl chain seems to be tolerated by Sirt5 at least in position 3 of glutaryl derivatives. Kinetic constants for **6e** and **6f** are similar to that of **6a**, and for **6g** similar to that for **6b**.

All compounds with methyl/hydroxyl substitutions are substrates for Sirt5 with K_M values in the low micromolar range but with dramatically reduced k_{cat} values. Determination of kinetic constants for the cosubstrate under saturating conditions for peptides **5a** and **5b** yielded very similar results (Figure S5) with NAD^+ K_M values of 29.6 ± 15.2 μM and 35.5 ± 11.7 μM, respectively, confirming that the additional

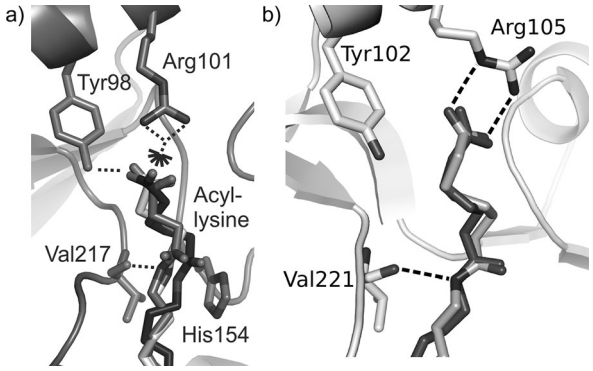

Figure 1. a) Crystal structures of zSirt5 with superposed **5a** (gray), **6a** (light gray), and **7** (dark gray). The protein is shown only once for clarity (zSirt5/**5a** complex; gray), since all protein residues superpose well. b) Docking of **8** (dark gray) and **9** (light gray) is only possible if Arg105 adopts another conformation that is also observed in the X-ray structure of PDB entry 3RIG. Polar interactions between ligand and protein are indicated as dashed lines.

methyl group in the acyl chain of the peptide substrate does not interfer with NAD^+ binding. Solving zSirt5 structures in complex with **5b** and **5c** reveals molecular reasons for this effect on k_{cat}. Compared to the structure with **5a**, the acyl side chain in **5b** and **5c** is twisted to position the hydrophobic methyl groups in appropriate active site cavities (Figure 2). This reorientation requires a rotation of the amide bond of the acylated lysine side chain, resulting in a carbonyl orientation that is probably not optimal for the nucleophilic attack at C1 of the ribose ring in the cosubstrate.

Determination of the respective K_D values using ITC yielded 830 ± 170 nM and 290 ± 40 nM for **5b** and **5c**, which is very similar to the K_D value for nonsubstituted parent peptide **5a**, indeed confirming that the unchanged K_M correctly indicates similar affinities to the active site. In contrast, substrate **5d** showed a 30-fold increased K_M value, likely due to the positive charge of the introduced primary amino function, since assuming that the binding is similar to that of **5b** would place this function in a hydrophobic environment. These results suggest the assumption that the chain length of the dicarbonic acyl residue as well as the orientation of the carboxyl group has a high impact on the k_{cat} value but less on the apparent affinity of the peptidic substrate.

Small acyl modifications can show significant effects on the substrate properties, suggesting the development of inhibitory binding groups: Exploiting the Sirt5 specific active site cavities should make it possible to further increase the binding affinity, in a nonproductive, inhibitory conformation, and it should enable isoform selective binding and inhibition.

We tested the idea of introducing bulkier acyl substituents to generate steric hindrance for NAD^+ binding by analyzing succinyl CPS1 derivatives with larger substitutions on C3 like **5j** and **5h**. These compounds could not be deacylated by the enzyme even when prolonged reaction times (up to 24 h) and higher Sirt5 concentrations (up to 2 μM) were used. Consistent with our hypothesis that they still bind to the active site of Sirt5 and block the NAD^+ site, these compounds are inhibitors for Sirt5 with K_i values of 100 ± 45 and 17.2 ± 1.3 μM for **5h** and **5j**, respectively (Table S2, Figures S6 and S7). Solving their complex structures with zSirt5 revealed that both modifications allow binding of the succinyl moiety like in substrate **5a**, and that these substitutions point toward the NAD^+ binding pocket (Figure S14a,b). Modeling NAD^+ from PDB ID 3RIY (Sirt5/succinyl-H3K9-peptide/NAD^+[13a]) into our zSirt5 structures shows that the modifications would clash with ribose atoms of the NAD^+ cosubstrate (Figure S18). For **5h** a mixture of *S* and *R* enantiomers appear to be bound, with slightly differing succinyl conformations but distal carboxyl groups and the phenyl moieties still in the same position. Our CPS1 derivatives thus reveal a novel principle for sirtuin inhibition based on peptides, which can also reveal valuable information for the development of small-molecule inhibitors.

Several sirtuin inhibitors, such as Ex527[15] and 4′-bromoresveratrol,[16] were recently shown to bind to the nicotinamide-accommodating C-site, indicating it as an attractive pocket for obtaining binding affinity. We therefore attempted to move the phenyl residue of **5h** deeper into the NAD^+ site, toward the C-site, by introducing a methylcarbamate linker between the succinyl and the phenyl group (**5i**). During the synthesis of this compound we were able to control the stereochemistry by using *Z*-protected aspartic acid derivatives in *S* and *R* configuration for the acylation reaction, yielding **5i** and **5o**, respectively. Testing benzyloxycarbonyl-protected aminosuccinyl derivatives showed that **5i** is an inhibitor for Sirt5 with about 3-fold improved K_i value (38.1 ± 0.6 μM) as compared to **5h** (Table S2). Peptide **5o** is an inhibitor with considerably reduced affinity to the active site of Sirt5 underlining the binding specificity for the *S* configuration. A crystal structure of the complex between **5i** and zSirt5 confirms that extending the linker in the *S* configuration moved the phenyl ring deeper into the C-site (Figure S14c). Only the methylcarbamate linker is well defined by electron density, while less pronounced spherical density is observed for the phenyl moiety in the C-site. The phenyl ring is in fact well positioned to mimic nicotinamide binding (Figure 3) but appears to be rotationally flexible, and adding a more nicotinamide-like carboxamide moiety to the phenyl ring is an obvious next step to improve binding of this acyl modification. Other large moieties can also be employed for binding to this active site region.

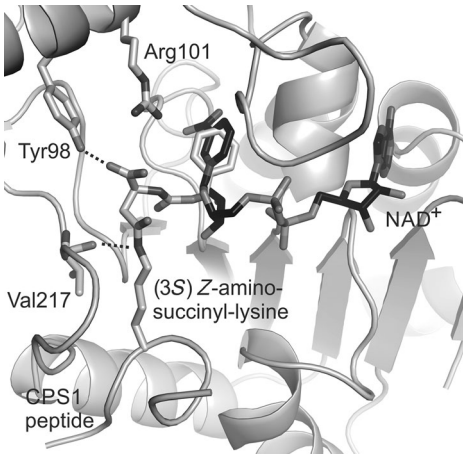

Figure 3. Crystal structure of zSirt5 active site with inhibitor **5i** (light gray). NAD^+ molecule was modeled in by an overlay with PDB entry 3RIG (dark gray). The protein is shown only once for clarity (zSirt5/**5i** complex; gray). Polar interactions between active-site residues and substrate peptides' acylated lysine are indicated by dotted lines.

Thus, introduction of a fluorenyl ring (**5p**) yielded an inhibitor with similar preference for the *S* configuration ($K_i = 46.0 \pm 0.23$ μM). Also, targeting additional active site areas could increase inhibitor affinity. Disubstitution at position 3 with a phenyl and a methyl moiety led to an about 20-fold increase in binding affinity of **5k** ($K_i = 4.3 \pm 0.32$ μM) compared to **5h**. Supposing that the observed orientation of **5h** for the phenyl group is similar, the methyl substituent at C3 can be assumed to occupy a position similar to the second methyl group in **5c** (Figure S10), indicating it as an interesting extension site for inhibitor development. Testing inhibition of human sirtuin isoforms by **5k** confirms that this approach achieved selectivity for Sirt5 versus Sirt1, 2, and 3 (Table S3).

Next steps in converting our peptide derivatives into small-molecule Sirt5 inhibitors comprise removal of the peptide part without losing sufficient affinity and replacement of the carboxyl moiety to enable membrane passage.

Substitution of the carboxyl group by a nitro function (**5l**) resulted in about 10-fold decrease of both K_M and k_{cat} values, that is, it is a well binding substrate. Crystal structure analysis of its zSirt5 complex shows that the nitropropionylated lysine indeed binds very similar to **5a** (Figure S13c).

Combining this nitro substitution with our novel acyl-based inhibition principle should now enable the systematic development of small-molecule inhibitors for Sirt5. This approach would lead to the first potent and selective Sirt5 inhibitors, which are anxiously awaited as research tools and as lead compounds for drug development.

Received: February 21, 2014
Published online: August 11, 2014

Keywords: acylation · inhibitors · protein deacetylases · Sirt5 · substrate specificity

[1] D. Rauh, F. Fischer, M. Gertz, M. Lakshminarasimhan, T. Bergbrede, F. Aladini, C. Kambach, C. F. Becker, J. Zerweck, M. Schutkowski, C. Steegborn, *Nat. Commun.* **2013**, *4*, 2327.

[2] A. A. Sauve, C. Wolberger, V. L. Schramm, J. D. Boeke, *Annu. Rev. Biochem.* **2006**, *75*, 435 – 465.

[3] a) M. C. Haigis, D. A. Sinclair, *Annu. Rev. Pathol.* **2010**, *5*, 253 – 295; b) S. Sanchez-Fidalgo, I. Villegas, M. Sanchez-Hidalgo, C. A. de La Lastra, *Curr. Med. Chem.* **2012**, *19*, 2414 – 2441; c) J. Schemies, U. Uciechowska, W. Sippl, M. Jung, *Med. Res. Rev.* **2010**, *30*, 861 – 889.

[4] a) Y. Chen, R. Sprung, Y. Tang, H. Ball, B. Sangras, S. C. Kim, J. R. Falck, J. Peng, W. Gu, Y. Zhao, *Mol. Cell. Proteomics* **2007**, *6*, 812 – 819; b) Z. Cheng, Y. Tang, Y. Chen, S. Kim, H. Liu, S. S. Li, W. Gu, Y. Zhao, *Mol. Cell. Proteomics* **2009**, *8*, 45 – 52; c) J. Garrity, J. G. Gardner, W. Hawse, C. Wolberger, J. C. Escalante-Semerena, *J. Biol. Chem.* **2007**, *282*, 30239 – 30245.

[5] M. Tan, H. Luo, S. Lee, F. Jin, J. S. Yang, E. Montellier, T. Buchou, Z. Cheng, S. Rousseaux, N. Rajagopal, Z. Lu, Z. Ye, Q. Zhu, J. Wysocka, Y. Ye, S. Khochbin, B. Ren, Y. Zhao, *Cell* **2011**, *146*, 1016 – 1028.

[6] C. Peng, Z. Lu, Z. Xie, Z. Cheng, Y. Chen, M. Tan, H. Luo, Y. Zhang, W. He, K. Yang, B. M. Zwaans, D. Tishkoff, L. Ho, D. Lombard, T. C. He, J. Dai, E. Verdin, Y. Ye, Y. Zhao, *Mol. Cell. Proteomics* **2011**, *10*, M111 012658.

[7] a) Z. Zhang, M. Tan, Z. Xie, L. Dai, Y. Chen, Y. Zhao, *Nat. Chem. Biol.* **2011**, *7*, 58 – 63; b) B. T. Weinert, C. Scholz, S. A. Wagner, V. Iesmantavicius, D. Su, J. A. Daniel, C. Choudhary, *Cell Rep.* **2013**, *4*, 842 – 851; c) G. R. Wagner, R. M. Payne, *J. Biol. Chem.* **2013**, *288*, 29036 – 29045.

[8] a) F. T. Stevenson, S. L. Bursten, R. M. Locksley, D. H. Lovett, *J. Exp. Med.* **1992**, *176*, 1053 – 1062; b) F. T. Stevenson, S. L. Bursten, C. Fanton, R. M. Locksley, D. H. Lovett, *Proc. Natl. Acad. Sci. USA* **1993**, *90*, 7245 – 7249.

[9] a) G. Boël, V. Pichereau, I. Mijakovic, A. Maze, S. Poncet, S. Gillet, J. C. Giard, A. Hartke, Y. Auffray, J. Deutscher, *J. Mol. Biol.* **2004**, *337*, 485 – 496; b) R. E. Moellering, B. F. Cravatt, *Science* **2013**, *341*, 549 – 553.

[10] a) M. Gertz, C. Steegborn, *Biochim. Biophys. Acta Proteins Proteomics* **2010**, *1804*, 1658 – 1665; b) H. Jiang, S. Khan, Y. Wang, G. Charron, B. He, C. Sebastian, J. Du, R. Kim, E. Ge, R. Mostoslavsky, H. C. Hang, Q. Hao, H. Lin, *Nature* **2013**, *496*, 110 – 113.

[11] A. Y. Zhu, Y. Zhou, S. Khan, K. W. Deitsch, Q. Hao, H. Lin, *ACS Chem. Biol.* **2012**, *7*, 155 – 159.

[12] J. L. Feldman, J. Baeza, J. M. Denu, *J. Biol. Chem.* **2013**, *288*, 31350 – 31356.

[13] a) J. Du, Y. Zhou, X. Su, J. J. Yu, S. Khan, H. Jiang, J. Kim, J. Woo, J. H. Kim, B. H. Choi, B. He, W. Chen, S. Zhang, R. A. Cerione, J. Auwerx, Q. Hao, H. Lin, *Science* **2011**, *334*, 806 – 809; b) J. Park, Y. Chen, D. X. Tishkoff, C. Peng, M. Tan, L. Dai, Z. Xie, Y. Zhang, B. M. Zwaans, M. E. Skinner, D. B. Lombard, Y. Zhao, *Mol. Cell* **2013**, *50*, 919 – 930.

[14] a) F. Fischer, M. Gertz, B. Suenkel, M. Lakshminarasimhan, M. Schutkowski, C. Steegborn, *PLoS One* **2012**, *7*, e45098; b) B. Maurer, T. Rumpf, M. Scharfe, D. A. Stolfa, M. L. Schmitt, W. He, E. Verdin, W. Sippl, M. Jung, *ACS Med. Chem. Lett.* **2012**, *3*, 1050 – 1053.

[15] M. Gertz, F. Fischer, G. T. Nguyen, M. Lakshminarasimhan, M. Schutkowski, M. Weyand, C. Steegborn, *Proc. Natl. Acad. Sci. USA* **2013**, *110*, E2772 – 2781.

[16] G. T. Nguyen, M. Gertz, C. Steegborn, *Chem. Biol.* **2013**, *20*, 1375 – 1385.

